

# **Numerical Prediction of Early-Age Cracking and Corrosion in High Performance Concrete Bridges – Case Study**

Lyne Daigle, P.Eng., M.Sc.  
Zoubir Lounis, P.Eng., Ph.D.  
Daniel Cusson, P.Eng., Ph.D.

Paper prepared for presentation

at the Innovations in Bridge Engineering Session

of the 2004 Annual Conference of the  
Transportation Association of Canada  
Québec City, Québec

## Abstract

This paper presents an evaluation of the effectiveness and the benefits of using high-performance concrete (HPC) containing corrosion inhibitors in the construction and repair of concrete bridges. Numerical models for predicting the early-age and in-service performance of HPC bridge structures are presented. The main parameters of these models, originally conceived for normal concrete, are revised and adapted for use with HPC containing corrosion inhibiting systems. The proposed models focus on the problems of early-age cracking, chloride ingress into concrete and corrosion of the conventional reinforcing steel. A case study of reinforced concrete (RC) barriers walls is used to illustrate the predictive capabilities of the models and the benefits of using HPC in extending the service life of bridge structures. Cost-effective mitigation measures for the prevention and control of cracking of HPC bridge structures are also suggested.

**Keywords:** high-performance concrete, bridges, chlorides, reinforcement corrosion, inhibitors, early-age cracking, in-service performance, service life.

## 1. Introduction

Concrete is the primary construction and repair material for many structural systems in Canada, such as highway bridges, high-rise buildings, parking structures, and dams. However, many of these structures, which have been exposed to aggressive environments, exhibit deterioration problems and fail to fulfill their design service life requirements. The major cause of degradation of reinforced concrete bridge structures in Canada and other countries is chloride-induced corrosion of the reinforcing steel. This problem can impair not only the serviceability of bridge structures but their safety as well. The cost of repair and rehabilitation of corrosion-damaged structures in North America is in the billions of dollars.

Deterioration of concrete due to corrosion presents considerable economic and technical challenges to bridge owners and engineers, specifically how to select the most appropriate design, protection system and rehabilitation strategy that extend the service life and reduce the life cycle cost of highway bridges. Different materials and protective systems have been used to extend the service life of concrete bridges, including high-performance concrete (HPC), corrosion inhibitors, epoxy coating, etc. The rehabilitation of concrete structures is a complex problem. Their field performance is difficult to predict, owing to the complexities associated with assessing material characteristics, environmental effects, damage initiation and accumulation, structural strength, failure mechanisms, and their impact on serviceability and safety. Other difficulties arise in detecting damage early in the life of the structure, and assessing the field performance of repaired concrete structures.

The development of innovative decision support tools is required to help bridge owners assess the condition and predict the performance of their structures. This will allow allocation of limited funds to achieve better overall management of the structures ensuring safety and durability at minimum life-cycle costs. To assist bridge owners and engineers in obtaining reliable information on early-age and in-service performance of concrete bridge structures, cost-effective condition assessment techniques and reliable models that predict early-age performance and durability of reinforced concrete in aggressive environments need to be developed.

In this paper, the benefits and shortcomings of HPC for use in the construction and rehabilitation of structures are summarized, along with proposed mitigative measures. The impact of

introducing corrosion inhibitors in concrete is discussed and numerical models that predict the performance of HPC bridge structures are presented. The models proposed will focus on the problems of early-age cracking, time-dependant chloride ingress into concrete, and onset of corrosion of conventional reinforcing steel. The prediction of damage resulting from corrosion, however, is outside the scope of the present paper. A case study of RC bridge barriers walls is used to illustrate the predictive capabilities of the models and the benefits of using HPC in extending the service life of bridge structures.

## **2. Performance of HPC Structures with Corrosion inhibitors**

In the literature, there are several definitions of HPC. In this paper, HPC refers to a concrete mix with a water-to-cementitious materials ratio (w/cm) of less than or equal to 0.4, with a permeability that can be 1 or 2 orders of magnitude lower than the permeability of normal concrete [1]. The main advantage of high-performance concrete lies in its great potential for ensuring adequate durability of concrete structures in aggressive environments. As corrosion of the steel reinforcement is a serious problem in most parts of the world, high-performance concrete as the potential to offer a cost-effective solution. Provided that cracking is prevented, the very low permeability of HPC can significantly delay the ingress of water and chlorides to the reinforcement, resulting in a much longer time to corrosion initiation compared to normal concrete [2]. Structures made of high-performance concrete may be designed to achieve higher strength and stiffness and/or superior durability compared to normal-strength concrete structures. The higher strength may allow the use of load-carrying and flexural members of reduced cross sectional areas and/or longer spans, which can result in larger usable floor areas in high-rise buildings and lighter superstructures in highway bridges.

### **2.1 Influence of cracking**

Despite the considerable research done, the impact of cracking on the corrosion of reinforcing steel remains a controversial issue [3]. On one hand, it is believed that cracks can reduce the service life of RC structures by accelerating the onset of corrosion and by promoting the active corrosion of the reinforcing steel through different mechanisms. It is recognized though that the premature onset of corrosion due to cracking is localized. On the other hand, the literature suggests that, since chlorides eventually penetrate the uncracked concrete after a few years and cause more widespread corrosion, the difference between cracked and uncracked locations is marginal. These conflicting viewpoints can be explained by the fact that the effect of cracking on the durability of concrete structures is a complex function of their type, width, depth and orientation. Studies have also shown that cracks with a width less than 0.3 mm have a marginal influence on the corrosion of reinforcing steel [3]. However, with the use of HPC that is more impermeable to water and chloride ingress than normal concrete, the difference in time-to-corrosion between uncracked and cracked locations is expected to be more significant in HPC structures.

High performance concrete can exhibit cracking at early ages, which has been observed in different bridge structures in North America [4]. Early-age cracking in HPC bridges is therefore a growing concern for their owners, as durability may be adversely affected. High-performance concrete does not in itself assure the durability of bridge structures. The use of appropriate construction techniques, to match the superior material properties inherent with this type of concrete, is also essential to improve concrete durability.

For an effective prevention or reduction of shrinkage, new admixtures and/or aggregates can be used in the preparation of HPC. They include: (i) shrinkage-reducing admixtures; (ii)

supplementary cementing materials (e.g. fly-ash or slag), as partial cement replacement and/or (iii) saturated lightweight aggregate, as a partial sand replacement, in order to reduce internal drying by releasing additional water to unhydrated cement particles. Shrinkage cracks can also be reduced or prevented at the design level by minimizing the degree of restraint in the concrete structure and thus reducing tensile stresses in concrete. Examples of mitigation measures include: (i) enhanced curing, (ii) smaller spacing of construction joints, (iii) better distribution of reinforcing steels, and/or (iv) reduced exposure to temperature extremes.

## **2.2 Role of corrosion inhibitors**

Corrosion inhibitors are chemical admixtures that are added to the concrete to prevent or delay corrosion of the embedded steel bars. They have been considered as one of the most user-friendly and cost-effective solutions to the wide spread problem of corrosion in RC structures and have been increasingly used in both new and existing reinforced concrete bridges during the last fifteen years. Corrosion inhibitors can influence the anodic or cathodic reaction, or both. Since both reactions must balance each other, a significant reduction in either one will result in a reduction in the corrosion rate. There are three main types of corrosion inhibitors: anodic, cathodic and organic. Anodic inhibitors act by forming an oxide film barrier on anodic surfaces of the reinforcing steel, increasing the level of chlorides needed to initiate corrosion. The most commonly used anodic inhibitor is calcium nitrite. Cathodic inhibitors form insoluble films on cathodic surfaces of the reinforcing steel and act as barriers to the reduction of oxygen. Organic inhibitors are adsorbed on the entire surfaces of the reinforcing bars and block both cathodic and anodic reactions. For most of these inhibitors, there are still very limited information on their long-term field performance [5].

## **2.3 Field performance monitoring and evaluation**

The field performance of concrete structures can be evaluated by periodic visual inspections of the concrete surface for early-age cracks, by the use of non-destructive evaluation (NDE) techniques and by continuous remote monitoring with embedded sensors. In field research, it is important to measure the key parameters at appropriate locations to allow a complete analysis of the problem at hand with as few assumptions as possible. While many types of sensors are available to measure the mechanical and thermal performance of concrete structures, sensors to detect chloride content are still to be developed. Corrosion activity can be evaluated by on-site NDE measurements of concrete electrical resistivity, electrochemical potential and rate of corrosion of the reinforcing steel [6].

Data obtained from the field, along with laboratory data, can be used to feed numerical models with realistic values of the governing parameters. Once calibrated with field and lab data, numerical models can be used to predict the performance of the structure under different loading and environmental conditions.

# **3. Numerical Models for Performance Prediction of HPC Structures**

## **3.1 Modeling of early-age structural performance and cracking**

A two-dimensional numerical model was developed to study the performance of HPC at early age using the ABAQUS finite element software package [7]. The analysis was conducted in three steps. The first step involved a thermal transient analysis to determine the temperature distribution in the concrete structure over time due to environmental factors such as, solar

radiation, wind cooling, ambient temperature (measured) and the internal heat generated by cement hydration. The governing equation is as follows:

$$D_T \left( \frac{\partial^2 T}{\partial x^2} + \frac{\partial^2 T}{\partial y^2} \right) + q = \frac{\partial T}{\partial t} \quad (1)$$

where  $D_T$  is the thermal diffusivity of concrete,  $q$  is the heat flux,  $T$  is temperature,  $t$  is time, and  $x$  and  $y$  are the distances through the thickness and height of the structure, respectively.

The second step involved the calculation of the time-dependant strains for drying shrinkage (RH measured) and autogenous shrinkage, as well as the measurement of traffic-induced vibration. The final step was a transient stress analysis of the individual strains that were added, taking into account the effect of time and temperature on the development (maturity) of strength and material properties, and the effect of creep on stress relaxation. The effect of cracking was also considered by updating the degree of restraint each time the tensile stress in concrete exceeded the calculated tensile strength. The stress  $\sigma$  at time  $t$  caused by a strain  $\varepsilon_R$  applied at time  $\tau$  was calculated by solving the following equation:

$$\sigma(t, \tau) = \int_{\tau}^t R(t, \tau) d\varepsilon_R(\tau) \quad (2)$$

where  $R(t, \tau)$  represents the stress produced at time  $t$  by a constant unit strain applied at time  $\tau$ .

It is known, however, that current design codes do not completely address the behaviour of concrete at early-age. Most existing models are based on either compressive test data or data on mature concrete, leaving a degree of uncertainty about modeling the field performance and cracking of concrete structures at early age. The above model can be used in a sensitivity analysis to assess the effect of introducing an error in the calculation of various concrete properties on total stress [8]. The main properties that should be tested are tensile strength, modulus of elasticity, maturity, thermal effects, shrinkage and creep.

### 3.2 Modeling of chloride ingress in concrete

Considerable research has been done over the last two decades to gain a better understanding of the mechanisms involved in the chloride-induced corrosion of reinforcing bars embedded in concrete. While most of the fundamental research was carried out in laboratories, many publications report field-simulated experiments and a limited number are based on actual field data [9-10-11]. As laboratory conditions cannot easily reproduce all the interrelated environmental conditions imposed on the structures, chloride ingress models should be based on field measurements and observations.

In this paper, Fick's second law of diffusion is used to model the chloride ingress into concrete. This model is generally accepted [1] to predict the chloride contamination of concrete bridge decks at different depths and times – corresponding to the initiation stage of the corrosion process [12]. Assuming that the concentration of chlorides on the surface is constant and the initial chloride content of the concrete mix is negligible, Crank's solution to Fick's 2<sup>nd</sup> law of diffusion yields [13]:

$$C(x,t) = C_s \left( 1 - \operatorname{erf} \left[ \frac{x}{2\sqrt{Dt}} \right] \right) \quad (3)$$

where  $C(x,t)$  is the chloride concentration at a depth  $x$  and time  $t$  ( $\text{kg}/\text{m}^3$ );  $C_s$  is the chloride concentration at the surface ( $\text{kg}/\text{m}^3$ );  $\operatorname{erf}$  is the statistical error function;  $x$  is the depth from the surface (m);  $D$  is the diffusion coefficient ( $\text{m}^2/\text{year}$ ) and  $t$  is the time of exposure to surface chlorides (years).

This equation would perfectly describe the diffusion of chlorides in a completely saturated homogenous material having a constant diffusion coefficient and where no other chemical reactions with chloride ions would occur. This is not the case in concrete structures. To predict chloride ingress in concrete structures the following issues should be considered:

- concrete is a heterogeneous material that can include cracks and micro-cracks;
- chloride concentration at the surface is known to vary with time and with the washing effect of rain;
- concrete surfaces of highway bridges are submitted to continual wetting and drying cycles;
- changing environmental conditions, such as temperature and humidity, affect the diffusion coefficient [14];
- hydration of cement paste is a chemical process that continues after the structure is put in service, especially for HPC with low  $w/cm$ . This chemical reaction has an influence on the diffusion coefficient [15]; and
- interface between cement paste and aggregates influence chloride diffusion [15].

Despite all these issues, the diffusion-based model was found to be the most appropriate one to describe a large number of chloride content profiles obtained from an extensive survey of different concrete structures in the USA [16]. The coefficient of diffusion found by regression analysis of the chloride profiles using equation (3) is referred to as the “apparent coefficient of diffusion” ( $D_{app}$ ), which includes the combined effects of the factors mentioned above. Similarly, the surface chloride concentration ( $C_s$ ) is also found by linear regression analysis.

### 3.2.1 Governing parameters and associated uncertainties

**Concentration of chlorides at the surface** – At some shallow depth, the chloride concentration reaches a maximum value and is considered to be quasi-constant [14, 17] after an initial time. This depth varies between 10 mm and 20 mm [18] depending on concrete quality and exposure conditions, with a value usually taken as 13 mm (1/2”) [16]. The *effective cover depth* is taken as the *concrete cover depth* less the *depth of maximum chloride concentration*. The chloride ingress is therefore modeled as a Fickian process over the effective cover depth.

The near-surface maximum chloride content (referred to as the surface chloride concentration in this paper) is known to be dependant on the severity of environment and type of exposure. For the chloride surface concentration, Weyers [16] has proposed some values based on the severity of the corrosive environment (Table 1). For the northeastern states of the USA, there seems to be a reasonably good relationship between the mean annual snowfall (MAS), the amount of deicing salts spread per kilometer of roads, and the surface chloride concentration [16]. For data collected in the New York state, the MAS varied between 0.95 to 2.9 m with an average of 1.95 m. For comparison, Table 2 gives the MAS for different cities in eastern Canada.

The types of exposure is often divided into three groups: (i) structures submerged in seawater or exposed to the seawater splash zone, (ii) structures above the seawater splash zone exposed to sprayed or atmospherically carried salts, and (iii) structures exposed to deicing salts used during winter seasons. The last category, which is the focus of our paper, can be further divided for different bridge elements. For a given bridge, the exposure to chlorides will be more severe on the deck, where the deicing salts are directly applied, than on the girders, piers and other elements with vertical surfaces such as barrier walls. One of the very few papers reporting measurements of surface chloride concentrations of a bridge deck and girders found that the  $C_s$  values for girders vary approximately between 10-25% of those measured on the bridge deck [19]. The bridge studied was in Minneapolis and exposed to a severe corrosive environment. For bridge barrier walls, a reduction factor of 50% is suggested as a first estimate since these elements are more directly submitted to traffic-induced spray of water and slush containing deicing salts than girders. Compared with the deck surface, the vertical orientation of the barrier surface increases washout of the surface chlorides thus supporting the use of a reduced value of  $C_s$ .

**Apparent chloride diffusion coefficient** – Coefficients of chloride diffusion into concrete measured in the laboratory have values that vary by more than one order of magnitude due to the diversity of mixes tested and difference in ages and curing conditions of the samples. The two variables recognized to have the most influence on the coefficient of diffusion were the water-cement ratio and the presence of mineral admixtures [1,16,20]. Taking a subset of the data found in the literature for  $w/cm \leq 0.40$  and samples older than 1 month, an average value of  $7.5 \times 10^{-5} \text{ m}^2/\text{year}$  with a coefficient of variation (COV) of 20% was found. This subset included some concrete samples with mineral admixtures. Table 3 shows a comparison of the different diffusion coefficients obtained with and without the addition of silica fume in the concrete mix. Other supplementary cementing materials such as fly ash and slag may also be used in HPC to help reducing the permeability of concrete and thus its chloride diffusion.

In a survey of bridges in 16 different states done by Weyers [16], field values of the apparent coefficient of diffusion were calculated from chloride content profiles. Average values of 9.7, 8.3 and  $7.1 \times 10^{-5} \text{ m}^2/\text{year}$  were reported for the Michigan, New York and Wisconsin states, respectively. Coefficients of variation were respectively 143%, 30% and 60%, including different types of concrete mixes. No specific sets of field data were found for a concrete with a low  $w/cm$ . Weyers further concluded that the corrosivity of the environment and time of exposure seemed to have a negligible effect on the apparent diffusion coefficient.

### 3.2.2 Modeling uncertainties in the chloride ingress model

Considering the limitation of the above deterministic model (Equation 3) to describe the complex chloride ingress mechanism and the large scatter and variability of the field data, the concepts of “apparent” chloride diffusion coefficient and “apparent” surface chloride concentration are employed to take into account some of the model uncertainty. To consider the inherent physical uncertainty of the model parameters, they are modeled as random variables with an average value, coefficient of variation (COV) and type of statistical distribution that are estimated from the field data and literature. Such modeling will enable the inclusion, in the model and parameters, of uncertainties, which will lead to more reliable prediction of the chloride concentration in concrete compared to the conventional deterministic model. Prediction of the actual distribution of chloride concentration at any given depth and time is obtained using Monte Carlo simulation. This method involves the random selection of a set of the input parameters according to their statistical distributions and calculation of the corresponding chloride concentration for specific depths and times. By repeating the process a large number of times with different random sets

of input parameters, a sample of solutions is obtained [21]. The results give a statistical distribution of chloride content as a function of time and depth. For the first estimation of chloride content, without chloride profile data available for the structure, the ranges of initial values for  $C_s$  and  $D_{app}$  are selected from the relevant data published in the literature (e.g. Tables 1 and 3). As chloride content profiles become available for the specific structure, the prediction model can be updated and refined by combining initial parameter estimations and field data.

### 3.3 Modeling of corrosion initiation of steel reinforcement

To predict the time of corrosion initiation ( $t_{co}$ ), the chloride concentration in equation (3) is set equal to a chloride threshold value  $C_{th}$  ( $\text{kg/m}^3$ ) at which corrosion initiation is expected to occur, and the variable  $x$  (the depth from the surface) is set equal to the effective cover depth of the reinforcing steel,  $d_c$  (m). Equation (3) is rewritten as follows:

$$t_{co} = \frac{d_c^2}{4D \left[ \text{erf}^{-1} \left( 1 - \frac{C_{th}}{C_s} \right) \right]^2} \quad (4)$$

#### 3.3.1 Governing parameters and related uncertainties

**Concrete cover** – The concrete cover thickness is at best known from construction records or estimated from NDE techniques (cover radar measurements). Even though cover thickness is usually taken as a constant value, it varies from one location to another and this variation is strongly related to the level of quality control during construction. In a detailed study [22] of the now demolished Dickson Bridge in Montreal, the concrete cover thickness was directly measured at numerous locations on the deck. The average cover depth was 36.6 mm with a COV of 45%. The specified design cover depth was 25 mm. It is therefore proposed to use values of coefficients of variation of 10%, 20%, and 30% (and beyond) for good, moderate, and low level of construction quality control, respectively.

**Chloride threshold** – The chloride threshold level is the concentration of chlorides necessary to break down the protective passive film on the reinforcing steel surface and initiate corrosion. As for the parameters previously discussed, chloride thresholds proposed in the literature cover a wide range of values. Glass and Buenfeld [23] discussed the different factors affecting the threshold value and gave a summary of reference values. The frequency distribution of the field chloride threshold values reported by Glass and Buenfeld are plotted in Fig. 1. The Rayleigh distribution was found to better describe the variability of these chloride threshold values with average value of 0.74% and a COV of 57%. The chloride threshold of 0.20% (of cement weight) proposed by the ACI Committee 222 is at the conservative end of the range whereas the value of 0.4% (of cement weight) used in Europe seems a more appropriate value [24].

The use of corrosion inhibitors, such as calcium nitrite, is recognised to have a retarding effect on the time to corrosion initiation [25,26]. The concentration of chlorides needed to initiate corrosion (chloride threshold) is increased as a function of the amount of calcium nitrite added. Precise values for the increased chloride threshold still need to be determined for long-term field exposure conditions. Indication of the level of protection (in terms of chloride concentration) offered by calcium nitrite inhibitor is presented in Table 4.

### 3.3.2 Modeling uncertainties in the corrosion initiation model

Similar to the prediction of chloride ingress into concrete, the prediction model for time to corrosion initiation is based on the Monte Carlo simulation method, which was described earlier. The results obtained from the Monte Carlo simulation give the probability of corrosion initiation at different points in time in the life of the structure. As for the prediction of chloride concentration, ranges of initial values for  $C_s$  and  $D_{app}$  are based on data published in the literature. The variability of the concrete cover depth is associated with the level of construction quality control. As field data are available for the specific structure, the prediction model can be updated and refined by combining initial parameter estimations and field data.

## 4. Case Study – Performance of HPC Bridge Barrier Walls

### 4.1 Rehabilitation work

In 1996, the normal-strength concrete barrier walls of the Vachon bridge in Laval (Québec) were rebuilt with high-performance concrete (HPC) due to extensive damage caused by corrosion, after 20 years of exposure to de-icing salts (Fig. 2a). The bridge had 21 simply supported spans of reinforced concrete slab on prestressed concrete girders. Ten 34-m spans of the barrier wall containing different types of corrosion inhibitors were fully instrumented [27] to evaluate their performance over a period of five years. The concrete used had a w/cm of 0.36, contained no mineral admixtures, had slumps near 75 mm, and air contents ranging from 6.5% to 7.0%. The complete mixture design is shown in Table 5. The corrosion inhibitors used were of all types: anodic, cathodic and organic, and some were combined with cementitious rebar coating, or surface-applied concrete coating or sealer [6]. Steel reinforcement consisted of eight 15-mm longitudinal bars in the wall cross-section and 15-mm transverse bars spaced at 230 mm along the wall length. Steel panel forms were used on the traffic-exposed face of the bridge barriers and plywood panels at the back. The upper surface of the barrier wall was covered with wet burlap until the forms were removed approximately 24 hours after the concrete was placed. The compressive strength obtained from concrete cores after 6 months had an average value of 45 MPa (ranging from 38 to 55 MPa). After 4.5 years, the average compressive strength increased by 30% due to continuous cement hydration up to 60 MPa (ranging from 50 to 69 MPa). As part of the evaluation and monitoring of the new barrier walls, chloride content profiles of ten sections, including a control one, were taken four times during the 5-year study.

### 4.2 Prediction of early-age cracking

An inspection of the barrier walls (36 hours after casting) revealed the presence of cracks traversing the complete depth of the walls. No joints other than the expansion joints between each 34 m long span were present to control cracking. Figure 2-b shows the uniform distribution of transverse cracks along the span of the barrier wall only 7 months after rehabilitation. The cracks had a width of 0.3 mm or less and average spacing of 0.8 m.

To study the roles and magnitude of the factors responsible for the observed cracking, the model presented before and described in more details in [7], on the early-age performance of HPC, was applied using the geometry and field data from the barrier walls. The computer simulation indicated that three series of cracking occurred in the first 3 hours after setting of concrete. Stress due to traffic vibration most likely played a role in the initial cracking at this early age. The last series of cracks was estimated to occur at 1.1 days. At this time, thermal stress was found to be the most important cause of cracking, followed by autogenous shrinkage.

Drying shrinkage was found to be negligible. The model estimated a final crack spacing of 1.1 m (L/32) at 1.1 days. Comparison with field observations is good with a crack spacing of 0.8 m measured at 1.5 days. The following conclusions were drawn from the analysis of cracking:

- Thermal stress, due to steep temperature gradients through the barrier wall, was the main factor responsible for the early-age cracking. Possible reasons are: significant heat of hydration due to the high cement content and very low w/cm of the mix; large thermal gradients because the front and back panels of the forms had different thermal properties; and thermal shock due to the premature removal of forms;
- Autogenous shrinkage of the low water-cement ratio (0.36) concrete seems to have contributed significantly to cracking;
- Dynamic deck deflection and resulting strain due to traffic vibration may have contributed to cracking at mid-span only, especially during the first hours after concrete setting when concrete was still very prone to cracking;
- Drying shrinkage was found to be negligible in the barrier wall, because of the short period of drying considered, the high density of the concrete, and the relatively large wall thickness.

In order to assess the effect of uncertainties in the calculation of different concrete properties on the total stress at early age, a 2D finite element model of the bridge barrier wall over the existing slab was run using actual field data. The sensitivity analysis indicated that the normalized stress (total stress divided by corresponding tensile strength) is much more sensitive to errors in predicting the modulus of elasticity and the tensile strength than to errors in predicting other properties, namely thermal, shrinkage and creep strains, and maturity. Therefore, future work on high-performance concrete at early-age ( $t < 7$  days) should focus on modeling tensile strength, and the modulus of elasticity under tensile loading.

#### 4.3 Prediction of chloride ingress

The mean annual snowfall in Montreal (Table 2) falls into the range measured in the New York state and, lacking more directly related data, the severity of the corrosive environment for a bridge in Montreal can be estimated to be similar to the level indicated for New-York. Barrier walls though, are not submitted to the same type of chloride exposure as bridge decks. An estimated reduction of 50% of the proposed  $C_s$  value of 7.36 ( $\text{kg}/\text{m}^3$ ) with a COV of 20% is taken for the surface chloride concentration (Table 1).

For the concrete mix used in the barrier walls (Table 5), an average value for the apparent coefficient of diffusion of  $7.5 \times 10^{-5} \text{ m}^2/\text{year}$  with a COV of 20% would be a reasonable first estimate as discussed earlier. The first two columns of data in Table 6 summarize the input parameters used for the numerical prediction model including the type of statistical distribution used in the Monte Carlo simulation.

The prediction of chloride content variations with depth is shown in Figs. 3a, 3b and 3c. With surface chloride concentration and diffusion coefficient values (and corresponding COV) taken from the literature, it is observed that the resulting range of chloride contents overestimate the chloride content of the barrier walls measured after 5 years (Fig. 3a).

The apparent coefficients of diffusion, surface chloride concentrations and depths of maximum chloride content were calculated from the field chloride profiles. The average apparent coefficient of diffusion is 25% lower than estimated from the literature data indicating that, after 5 years, the field performance of HPC in terms of chloride diffusivity is better than expected. The low COV of 20% obtained for the test sections with and without corrosion inhibitors indicates that the addition of corrosion inhibitors did not significantly affect the apparent coefficient of diffusion,

as expected. The concentration of surface chlorides is also lower than first estimated with a reduced COV. The variability of the depth of maximum chloride content is considered by using the calculated mean and COV values instead of a fixed depth as in the first estimate.

A better match between the model prediction and the measured chloride profiles is obtained when the surface chloride concentration and diffusion coefficient are taken from the field data obtained at the Vachon bridge (Fig 3b). In that case though, the prediction relies on data taken at only one point in time (since only the Year-5 profiles were considered). In this case study, equal importance is given to data from literature and the field measurements obtained after five years. The updated input parameters were obtained by combining literature-estimated data with the parameters obtained from the field (Table 6). The range of chloride concentration prediction, based on updated parameters, fits better the measured chloride profiles than the prediction obtained with the initial parameter values, especially for larger cover depths (Fig. 3c). The model prediction would be further improved by updating the input parameters with subsequent chloride profile measurements.

The prediction of the chloride content of the barrier walls after 50 years is shown in Fig. 4. On the vertical axis (right-hand side), different values of chloride threshold are indicated in % of cement weight. At the depth of the reinforcing steel, the only chloride threshold that would be exceeded after 50 years is the 0.2% value specified by ACI which is, as mentioned before, on the conservative side.

#### **4.4 Prediction of corrosion initiation**

The concrete cover thickness of the barrier walls was measured at two locations for each section. A minimum design thickness of 75 mm was specified; an average thickness of 90 mm was measured with a COV of 16%. This variation corresponded to a good-to-moderate construction quality control.

In uncracked concrete, the prediction of corrosion initiation is highly dependent on the chloride threshold value used in the model (Fig. 5). For instance, at 30% probability of corrosion (i.e. 30% of the reinforcing steel would have started to corrode), a chloride threshold value of 0.2% by cement weight gives a time to corrosion initiation of 30 years (24 years for the first estimate). For the same probability, a threshold level of 0.4% results in an estimated time to corrosion initiation of 96 years (65 years for the first estimate), which is well beyond the design service life of barrier walls. For the threshold levels measured in the field, the estimated time to corrosion initiation for a 30% probability of corrosion is over a hundred years. The probability of corrosion initiation is more conservative in the first case. The chloride threshold obtained from field data is described by an average value and a coefficient of variation whereas chloride thresholds of 0.2% and 0.4% are single deterministic values.

Presenting the time to corrosion initiation in terms of probability of corrosion better reflects the fact that corrosion onset will not occur uniformly, or at the same time, on the reinforcing steel of the entire structure. As observed by the variability of the field input parameters, local variations due to external and internal factors are always present.

#### **4.5 Evaluation of corrosion inhibitors based on corrosion rates**

The performance of the different corrosion inhibitors used at the Vachon bridge was evaluated with two non-destructive methods, the half-cell potential and the corrosion rate measurements. Only the latter is discussed here. During reconstruction of the barriers, special reinforcing steel

bars were installed at 25 mm from the concrete surface to allow an earlier assessment of the performance of the corrosion inhibiting systems. Results of the corrosion rate measurements taken on these rebars after five years are shown in Fig. 6. The five sections that only had corrosion inhibitors as a protective system against corrosion showed the lowest corrosion rate ( $< 0.17 \mu\text{A}/\text{cm}^2$ ) with a chloride content that did not exceed 0.41% of cement weight. Higher corrosion rates were measured for other systems, ranging from 0.27 to  $0.41 \mu\text{A}/\text{cm}^2$ . From this set of measurements taken over 5 years, the corrosion inhibitors used alone seemed to perform better than the other protective systems tested.

One of the corrosion inhibitors tested was calcium nitrite. Assuming that the lowest recommended dosage was used, the associated chloride threshold would be 1.0% of cement weight (Table 4). The corrosion rate was equivalent or less for three of the other corrosion inhibitors tested. Estimating the corrosion onset of these four sections against a chloride threshold value of 0.4% (of cement weight) would still be on the conservative side provided their inhibitive properties remain as effective with time. The results of the numerical prediction clearly show that if a chloride threshold value of 0.4% can safely be used in the presence of corrosion inhibitors, the predicted service life of concrete structure is greatly extended (Fig. 5).

The corrosion rate at cracked and uncracked locations was measured for the main reinforcing steel installed at the design cover depth of 75 mm. For the control section and the sections containing corrosion inhibitors, corrosion rates were higher at cracked locations except for one case where the corrosion rate was slightly lower (5%). The increase in corrosion rate was between 20% and 80%, showing that 0.3 mm wide cracks can in fact affect the corrosion rate to some extent. The monitoring of the corrosion rate with time at cracked and uncracked locations will enable further confirmation of the effect of early-age cracking on the corrosion process. With the predicted time to corrosion initiation being so high for a 30% probability of corrosion (i.e. 30 and 96 years for chloride thresholds of 0.2% and 0.4%, respectively), the extensive early-age cracking observed at the bridge will most likely have a strong influence on the corrosion resistance of the barrier walls. It is therefore clear that the effect of early-age cracking in HPC structures will have to be considered in corrosion initiation models.

## 5. Conclusions

Through the use of numerical prediction models, the case study presented in this paper confirmed the effectiveness and benefits of using HPC containing corrosion inhibitors for the rehabilitation of corrosion-damaged bridge barrier walls. Provided appropriate construction techniques are used to prevent early-age cracking, the estimated time to reach a certain probability of corrosion was found to be quite long, which will lead to an extended service life of the barrier walls. The low chloride permeability of HPC, combined with a more confident use of a higher chloride threshold level due to the presence of inhibitors, contributed to this enhanced resistance to chloride ingress and corrosion. The following conclusions are drawn from the use and application of the numerical prediction models:

- The autogenous shrinkage of concrete with low water-cement ratio seems to contribute significantly to cracking which could potentially affect the corrosion resistance of HPC containing corrosion inhibitors;
- For a specific concrete structure, the variability in time and space of the governing parameters involved in chloride diffusion and reinforcing steel corrosion cannot be ignored;

- The variability of the parameters that strongly influence the outcome of the diffusion model is best accounted for by using an approach that takes uncertainties into consideration. Numerical simulation is a practical and reliable technique to achieve this objective;
- The input parameters, each described by an average value, a coefficient of variation and statistical distribution can be best obtained from a combination of sources, such as: relevant field data, literature data and expert opinion;
- The presentation of the time to corrosion initiation in terms of probability of corrosion better reflects the fact that the onset of corrosion will not occur uniformly, at the same time, on the reinforcing steel for the entire bridge structure;
- As field monitoring of concrete structures progresses, data on surface chloride concentration, chloride profiles and corrosion rate measurements will become more readily available. A larger database will then enable the selection of better estimates of input parameters for the proposed models and refine the earlier predictions; and
- The effect of early-age cracking in HPC structures will have to be considered in future chloride ingress and corrosion prediction models.

## 6. Acknowledgment

The authors wish to acknowledge Ministère des transports du Québec and the product suppliers for their contributions to the field investigation of the Vachon Bridge.

## 7. References

1. Tang, L, and Nilsson, L.-O. 1992. Chloride Diffusivity in High Strength Concrete at Different Ages. Nordic Concrete Research, Pub. No. 11 (1), 162-171.
2. Neville, A.M. 1996. Properties of concrete, 4th ed., Longman Group Limited, Essex, pp. 844.
3. ACI Committee 222. 1996. Corrosion of metals in concrete. ACI 222R-96, American Concrete Institute, Detroit, MI, pp. 30.
4. TRB. 1996. Transverse Cracking in Newly Constructed Bridge Decks, National Co-operative Highway Research Program Report 380, Transportation Research Board, National Academy Press, Washington, pp. 126.
5. Virmani, Y.P. and Clemana, G.G. 1998. Corrosion Protection – Concrete Bridges. FHWA-RD-98-088, Federal Highway Administration.
6. Qian, S.Y. and Cusson, D. 2004. Electrochemical Evaluation of the Performance of Corrosion-Inhibiting Systems in Concrete Bridges, Cement & Concrete Composites, Vol. 26, pp. 217-233.
7. Cusson, D. and Repette, W. 2000: «Early-Age Cracking in Reconstructed Concrete Bridge Barrier Walls, » ACI Materials Journal, 97(4), July/August, pp. 438-446.
8. Cusson, D. 2001. Sensitivity Analysis of the Early-Age Properties of High-Performance Concrete - A Case Study on Bridge Barrier Walls, Creep, Shrinkage & Durability Mechanics of Concrete and Other Quasi-Brittle Materials Conference, Cambridge, pp. 325-330.
9. Paulsson-Tralla, J. and Silfwerbrand, J. 2002. Estimation of Chloride Ingress in Uncracked and Cracked Concrete Using Measured Surface Concentrations. ACI Materials Journal. Vol. 99, pp.27-36.
10. Lounis, Z. 2003. Probabilistic Modeling of Chloride Contamination and Corrosion of Concrete Bridge Structures. Proc. of Int. Symp. on Uncertainty Modeling and Analysis, College Park, MD., Sept. 21-24 2003, pp. 447-451.
11. Goltermann, P. 2003. Chloride Ingress in Concrete Structures: Extrapolation of Observations. ACI Materials Journal, Vol. 100, pp. 114-119.

12. Tuutti, K. 1982. Corrosion of Steel in concrete (tech. Rep.) Stockholm: Swedish Cement and Concrete Research Institute, pp. 469.
13. Crank, J. 1975. The Mathematics of Diffusion (2<sup>nd</sup> ed.). London, Oxford University Press.
14. Martin-Pérez, B. 1999. Service Life Modelling of R.C. Highway Structures Exposed to Chlorides. Ph.D. Thesis, Department of Civil engineering, University of Toronto, pp.168.
15. Xi, Y. and Bazant, Z.P. 1999. Modeling Chloride Penetration in Saturated Concrete. Journal of Materials in Civil Engineering. Vol. 11. No.1, pp. 58-65.
16. Weyers et al. 1994. Concrete Bridge Protection and Rehabilitation: Chemical and Physical techniques. Service Life Estimates. SHRP-S-668. National Research Council, Washington.
17. Tuutti, K. 1993. The Effect of Individual Parameter on Chloride Induced Corrosion. In L.-O. Nilsson (Ed.), Chloride Penetration into Concrete Structures (pp.18-25). Göteborg, Sweden.
18. Andrade, C., and Alonso, C. 1996. Progress on Design and Residual Life Calculation with Regard to Rebar Corrosion of Reinforced Concrete. In N. Berke, E. Escalante, C.Nmai and D. Whiting (Eds.), Techniques to Assess Corrosion Activity of Steel Reinforced Concrete Structures, ASTM STP 1276, pp.23-40.
19. Coggins, F. and French, C. 1990. Chloride Ion Distribution in Twenty-Year Old Prestressed Bridge Girders. ACI Materials Journal. Vol. 87, No. 5, pp. 479-488.
20. Pedersen, V., and Arntsen, B. 1998. Effect of Early-age Curing on Penetration of Chloride Ions Into Concrete in the Tidal Zone. Proc. of the 2<sup>nd</sup> Intl. Conf. on Concrete under Severe Conditions, CONSEC '98, Tromso, Norway, June 21-24, 1998, pp. 468-477.
21. Ang, A.H-S. and Tang, W.H. 1984. Probability Concepts in Engineering Planning and Design. Vol II – Decision, Risk, and Reliability. John Wiley & Sons, Inc. New-York.
22. Lounis, Z. and Amleh, L. 2003. Reliability-Based Prediction of Chloride Ingress and Reinforcement Corrosion of Aging Concrete Bridge Decks, Proceeding of the 3<sup>rd</sup> International IABMAS Workshop on Life-Cycle Cost Analysis and Design of Civil Infrastructure Systems, Lausanne, Switzerland, pp. 139-147.
23. Glass, G.K. and Buenfeld, N.R. 1997. Chloride Threshold Levels for Corrosion Induced Deterioration of Steel in Concrete. Chloride Penetration into Concrete: St-Remy-les-Chevreuses, France, October 15-18, 1995. Proc. of the RILEM Intl. Workshop, pp. 429-452.
24. Comité Euro-International du béton. 1992. Durable Concrete Structures. Design Guide. 2<sup>nd</sup> edition. Thomas Telford ed. Bulletin d'information no. 183.
25. Berke, N.S. and Hicks, M.C.2004. Predicting Long-term Durability of Steel Reinforced Concrete with Calcium Nitrite Corrosion Inhibitor. Cement Concrete and Composites. Vol. 26, pp.191-198.
26. Bentur, A., Diamond, S. and Berke, N.S. 1997. Steel Corrosion in concrete. E & FN Spon, (Chapman & Hall) London, UK.
27. Cusson, D. and Mailvaganam, N.P. 1999. Monitoring and Evaluation Techniques: Corrosion-Inhibiting Systems in Reconstructed Bridge Barrier Walls. Concrete International, Vol. 21, No. 8, pp. 41-47.
28. El-Jazairi, B. And Berke, N.S. 1990. The Use of Calcium Nitrite as a Corrosion Inhibiting Admixture to Steel Reinforcement in Concrete. In "Corrosion of Reinforcement in Concrete", eds C.L. Page, K.W.J. Treadaway & P.B. Bamforth. Society of Chemical Industry, Elsevier Applied Science, pp. 571-597.
29. Millard, S.G. 1993. Corrosion Rate easurement of In-Situ Reinforced Concrete Structures. Proc. ICE, Structs and Bldgs, Vol 99. Feb. 1993, pp. 84-88.

## Tables

Table 1. Severity of corrosive environments for bridge decks (Weyers et al. 1994)

Severity level	Mean $C_s$ value ( $\text{kg/m}^3$ )	Range of $C_s$ values ( $\text{kg/m}^3$ )	Regions
Low	1.78	0 – 2.4	Kansas
Moderate	3.56	2.4 – 4.7	Florida
High	5.34	4.7 – 5.9	West Virginia, Iowa
Severe	7.36	5.9 – 8.9	New York

Table 2. Mean annual snowfall for selected Eastern Canadian cities

Cities	Mean annual snowfall (m)
St. John's (NF)	3.59
Charlottetown	3.30
Halifax	2.71
Saint John (NB)	2.92
Sept-îles	4.26
Montreal	2.35
Toronto	1.31

Table 3. Diffusion coefficients of HPC with and without the addition of silica fume

w/cm	OPC ( $\text{kg/m}^3$ )	SF ( $\text{kg/m}^3$ )	Sample age (months)	Diffusion coef. ( $\times 10^{-5} \text{ m}^2/\text{year}$ )	Reported by
0.40	420	-	54	5.4	Pedersen and Arntsen [20]
0.40	389	31.1 (8%)	54	1.3	Pedersen and Arntsen [20]
0.32	522	-	6	5.5	Tang and Nilsson [1]
0.32	492.5	29.5 (6%)	6	1.2	Tang and Nilsson [1]
0.32	466	56 (12%)	6	0.7	Tang and Nilsson [1]

Table 4. Calcium nitrite protection against chloride-induced corrosion  
(modified from El-Jazairi et al. [28])

Calcium Nitrite Content (kg/m <sup>3</sup> , 30% solid)	Chloride content at steel level (kg/m <sup>3</sup> )	Corresponding chloride threshold (% cement wt.)
10	3.6	1.0 *
15	5.9	1.7 *
20	7.7	2.2 *
25	8.9	2.5 *
30	9.5	2.7 *

\* Based on case study mix

Table 5. Mixture design of barrier wall concrete

Constituents	Quantity per m <sup>3</sup>
Crushed stone, 20 mm	361 kg
Crushed stone, 14 mm	361 kg
Crushed stone, 10 mm	309 kg
Sand	702 kg
Cement (ASTM Type 1)	450 kg
Water	160 kg
Water reducer	1125 ml
Air entrainer	315 ml
Superplasticizer	1500 ml
w/cm	0.36
Corrosion inhibitors (for selected sections)	Varied with products

Table 6. Model input parameters

Parameter	Initial parameter (from literature)		Field data (case study)		Updated parameter		Statistical distribution
	Mean	COV (%)	Mean	COV (%)	Mean	COV (%)	
Cover depth (mm)	90.8 (measured)	16 (measured)	90.8	16	90.8	16	Normal
Surface chlorides (kg/m <sup>3</sup> )	3.68	20	2.77	13	3.21	15	Normal
Apparent diffusion coefficient (m <sup>2</sup> /s)	7.5e-5	20	5.6e-5	20	6.5e-5	20	Lognormal
Depth of maximum chloride content (mm)	13	fixed	15.6	30	15.6	30	Lognormal

## Figures

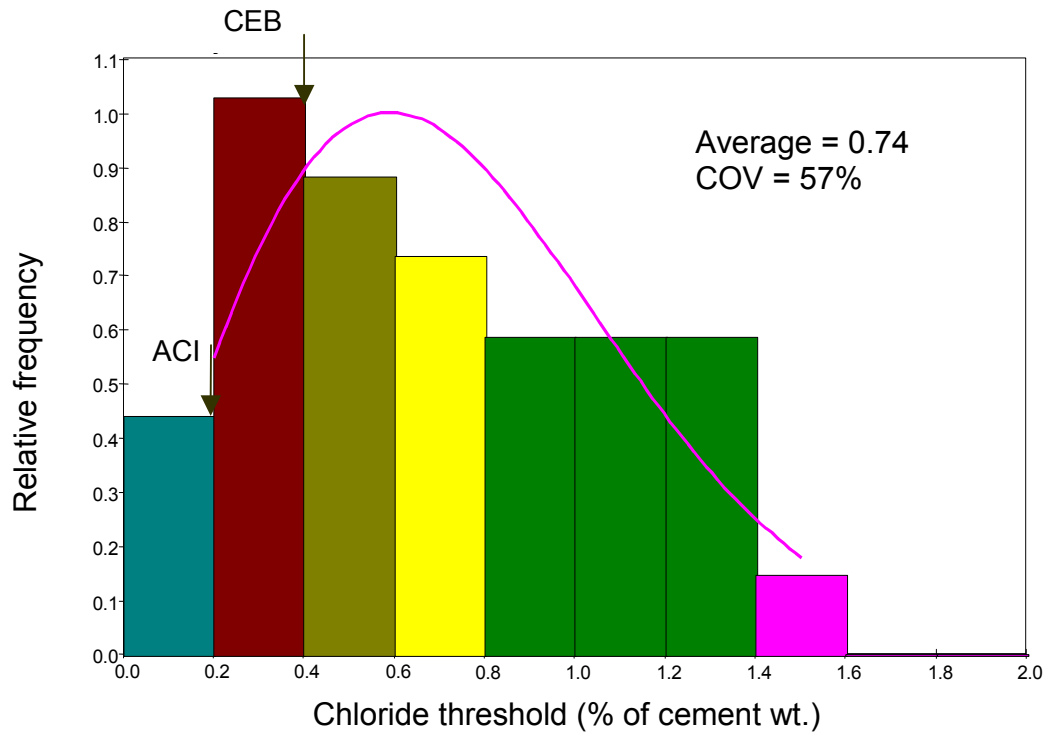


Figure 1. Distribution of field chloride threshold level from the literature

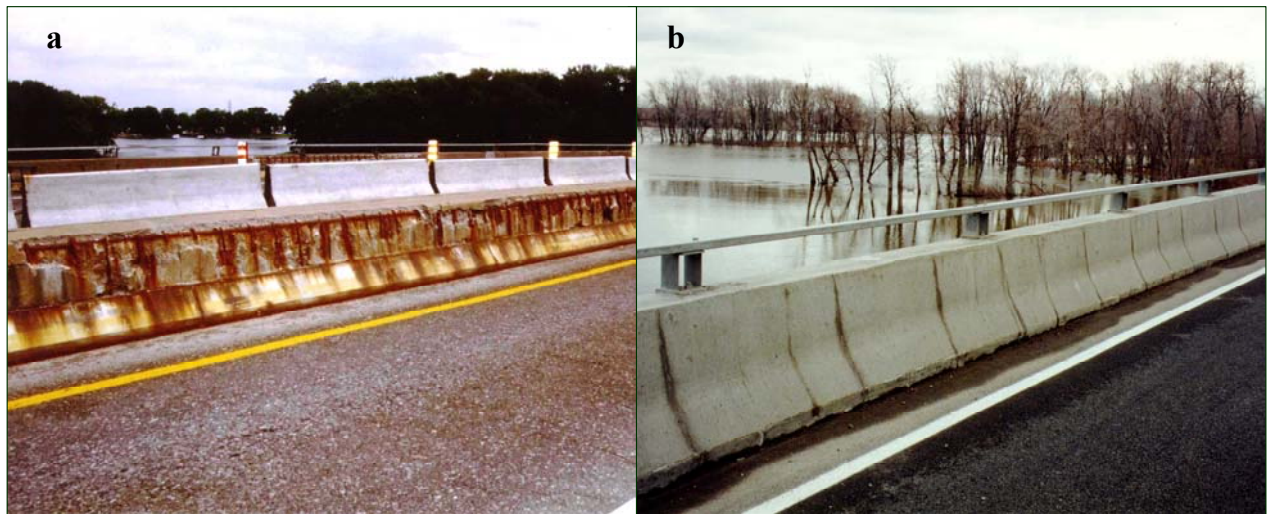


Figure 2. Vachon bridge barrier walls: (a) severe corrosion damage prior to rehabilitation in 1996 and (b) early-age cracking after rehabilitation

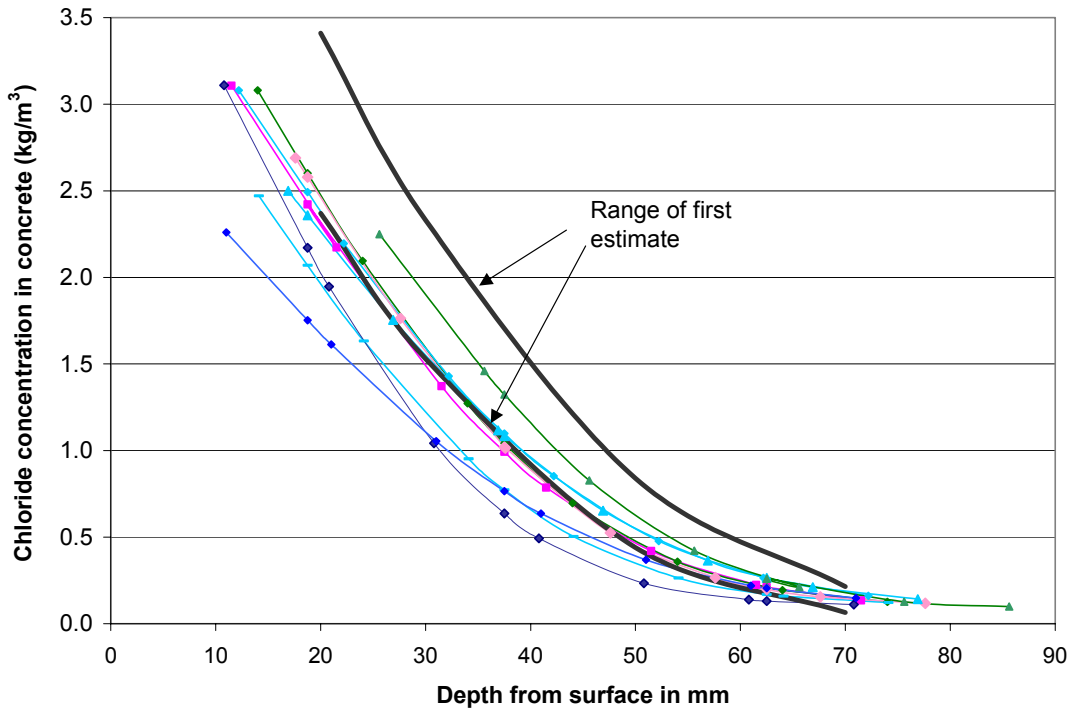


Figure 3a. Chloride profiles in the barrier wall after 5 years – first estimate

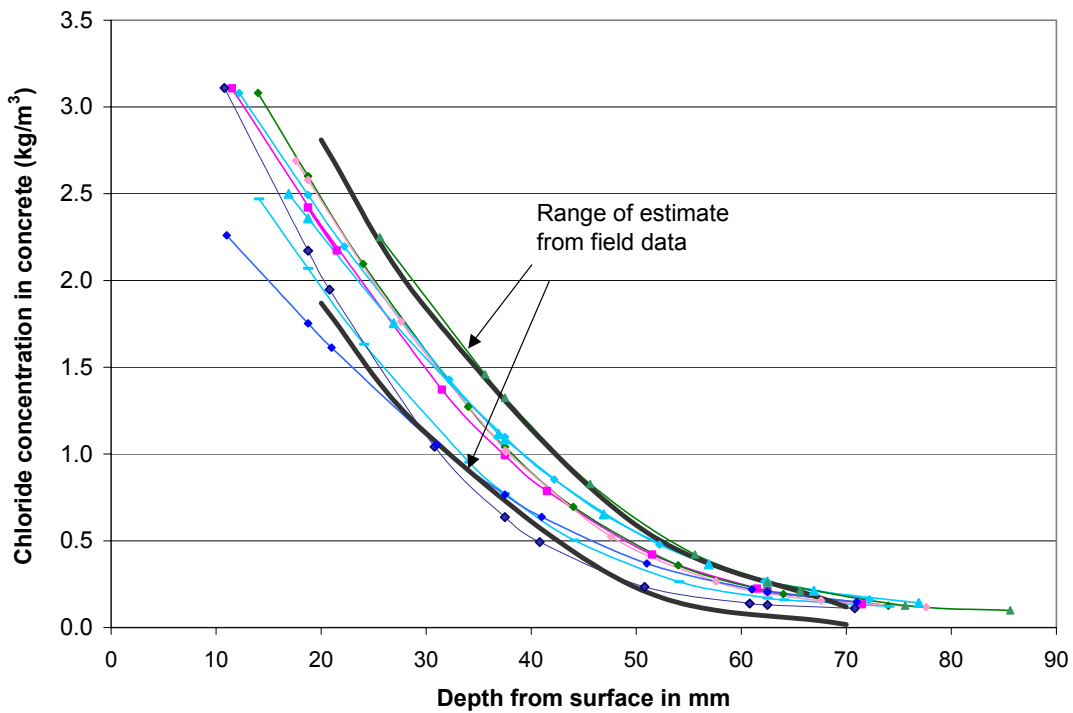


Figure 3b. Chloride profiles in the barrier wall after 5 years – input parameter from field measurements

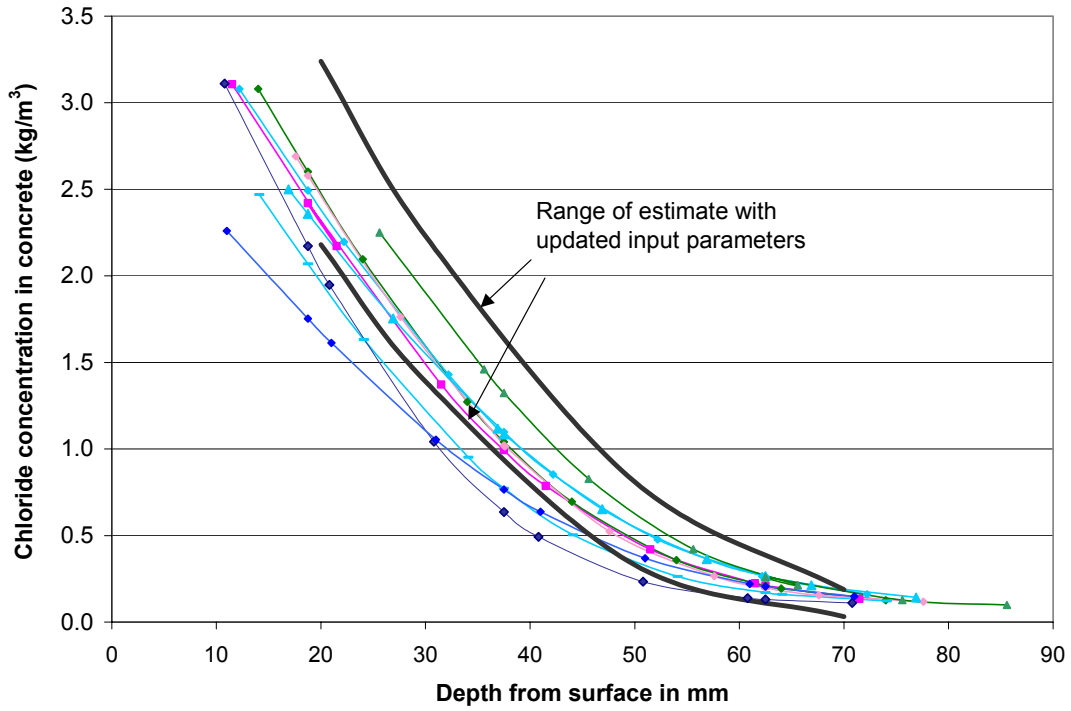


Figure 3c. Chloride profiles in the barrier wall after 5 years – updated estimate

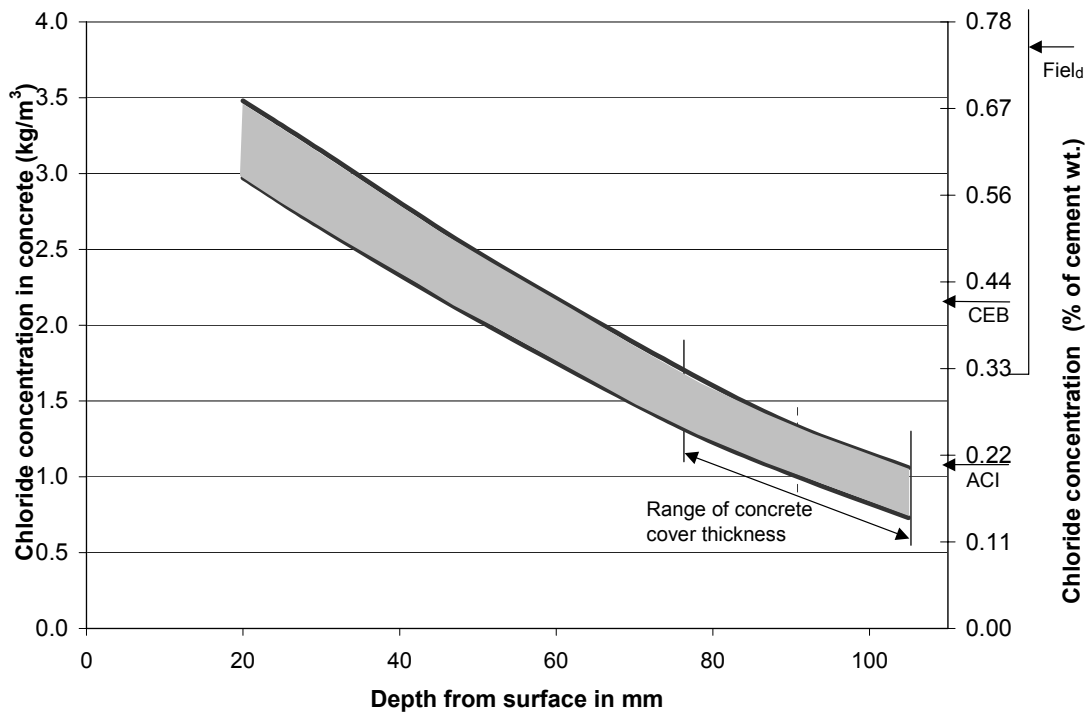


Figure 4. Prediction of chloride content in the barrier walls after 50 years

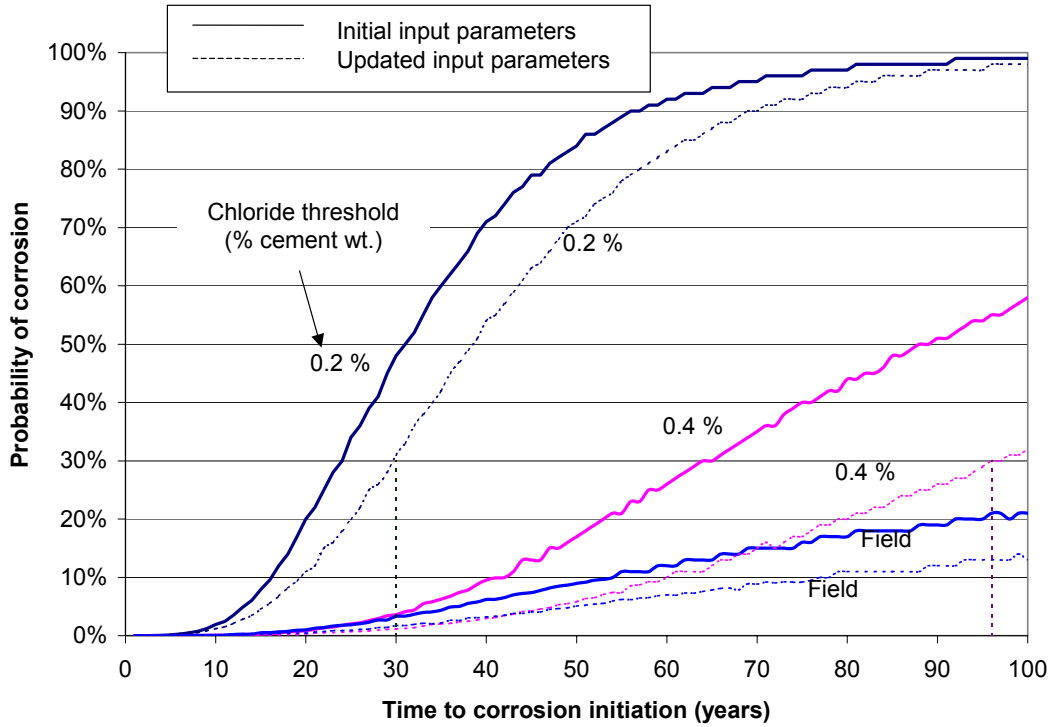


Figure 5. Case study – Prediction of time-dependent probability of corrosion

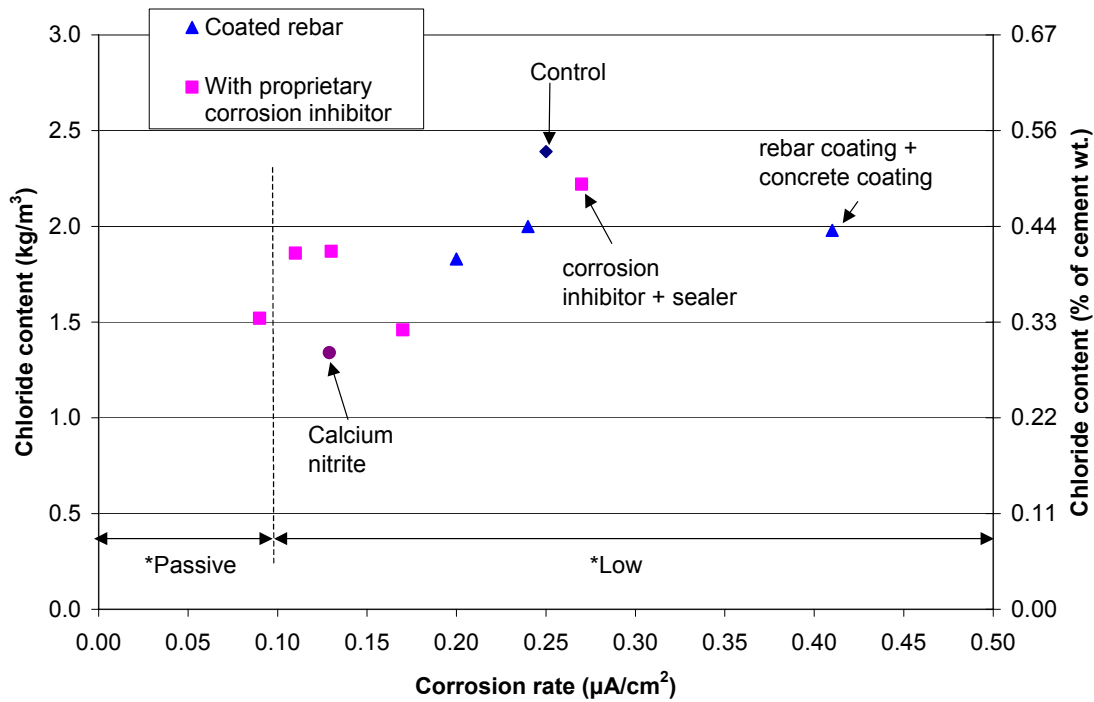


Figure 6. Corrosion rate after five years on special reinforcing bars installed at 25 mm depth. (\* Typical ranges of corrosion rate defined according to Millard [29])